

Quantum-chemical study of the Lewis acid influence on the cycloaddition of benzonitrile oxide to acetonitrile, propyne and propene

Gabriele Wagner,^{a,*} Timothy N. Danks^b and Vincenzo Vullo^a

^aChemistry Division, SBMS, University of Surrey, Guildford, Surrey GU2 7XH, United Kingdom

^bThe Oratory School, Woodcote, Reading, Berkshire RG8 0PJ, United Kingdom

Received 17 November 2006; revised 13 March 2007; accepted 29 March 2007

Available online 4 April 2007

Abstract—Quantum chemical methods (MP2 and B3LYP) together with a topological analysis of the charge density have been used to study the BH_3 - or BF_3 -mediated reaction of benzonitrile oxide with acetonitrile, propyne and propene. In the reaction with propene or propyne, addition of Lewis acids has only little influence on the outcome of the reactions. The cycloaddition of nitrile oxides with nitriles, however, is generally promoted by strong Lewis acids. When the Lewis acid coordination takes place at the nitrile oxide the reactant is activated and the product binds weakly to the Lewis acid so that the reaction is expected to be catalytic. In the case of coordination to the nitrile the reaction is Lewis acid mediated. Here the reactant is not much influenced by addition of Lewis acid, but the transition state and the product are stabilised and consequently such processes require a stoichiometric amount of Lewis acid and form a stable Lewis acid–product complex. It has also been demonstrated that the different activation routes for these reactions involve different reaction mechanisms. Whereas the reaction of a Lewis acid coordinated nitrile oxide is of ‘inverse electron demand’, the Lewis acid coordinated nitrile reacts through a ‘normal electron demand’ cycloaddition.

© 2007 Elsevier Ltd. All rights reserved.

1. Introduction

Cycloadditions are of high practical use in the synthesis of heterocycles, due to their complete atom economy and high functional group compatibility.¹ Nitriles, however, although promising starting materials for a number of nitrogen containing heterocycles, have been rarely employed in cycloadditions because of their low reactivity in such type of reactions.²

In our previous work, we found that nitrile-specific Lewis acids such as Pt(IV), Pt(II) or Pd(II) facilitate the cycloaddition of nitrones to coordinated nitriles. These metal mediated reactions occur under mild conditions and with a wide range of nitriles. They afford Δ^4 -1,2,4-oxadiazolines, which are difficult to prepare using other methods, or not accessible at all.³ A quantum chemical study showed that the purely organic reaction is a concerted pericyclic reaction with a high activation barrier and a low thermodynamic driving force. In terms of orbital interactions, the reaction can be classified as one of the ‘normal electron demand’, i.e., an occupied

orbital of the dipole interacts with an unoccupied one of the dipolarophile. Coordination of the nitrile to a model Lewis acid changes the reaction mechanism towards a two-step reaction. The Lewis acid activates the starting material only poorly, but rather acts by stabilising the highly polar transition states and intermediates, as well as the product.⁴ Due to the strong interaction of the Lewis acid with the product, the reaction is not catalytic.

In our attempts to extend the chemistry of nitriles towards cycloadditions with other dipolar reagents, we examined the mechanism of the reaction of acetonitrile with benzonitrile oxide.⁵ This work demonstrated that the Lewis acid free reaction differs mechanistically from the corresponding reaction with nitrones, in that an interaction of an occupied orbital of the nitrile with an unoccupied one of the benzonitrile oxide is now relevant for the bond formation. The reaction is of ‘inverse electron demand’. In this light, Lewis acid coordination to the dipole is expected to accelerate the reaction, whereas coordination to the nitrile should retard it. Experimental data, however, point to an enhanced reactivity of electron deficient nitriles,⁶ and this apparent contradiction suggests that the system can easily switch between inverse and a normal electron demand. Under these circumstances, coordination of a Lewis acid to the nitrile might also promote the reaction, by changing its mechanism.

Keywords: Cycloaddition; Lewis acid; Ab initio calculations; Topological analysis; Catalysis.

* Corresponding author. Tel.: +44 (0) 1483 686831; fax: +44 (0) 1483 686851; e-mail: g.wagner@surrey.ac.uk

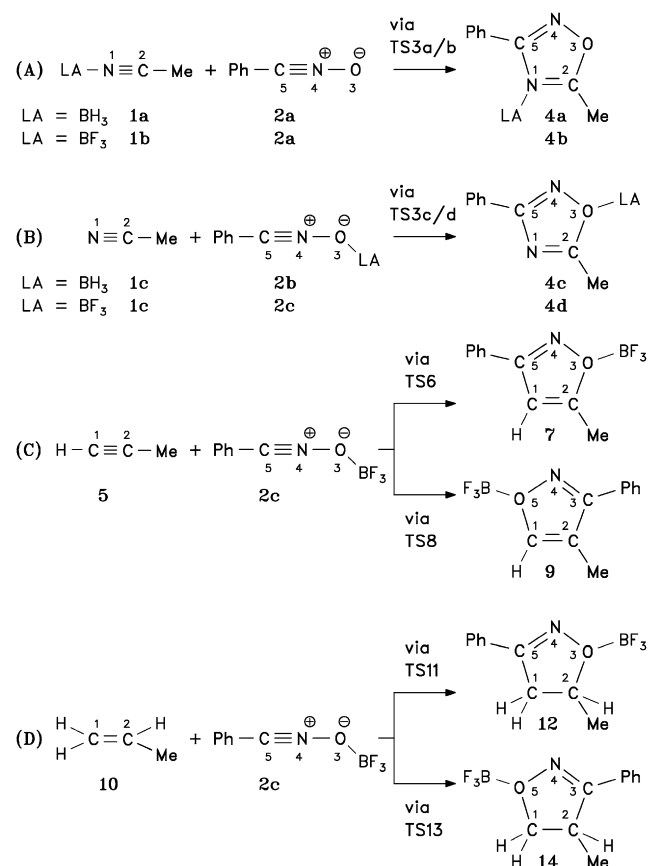
In order to verify this hypothesis, we have now used quantum mechanical calculations together with a topological analysis of the charge density to study the two possible reaction pathways of the Lewis acid mediated reaction of acetonitrile and benzonitrile oxide. As examples of a strong and a weak Lewis acid BF_3 and BH_3 have been chosen. The results are compared with the Lewis acid free reaction, in terms of relative energies and orbital involvement. Questions such as which activation pathway is more efficient, and which one is experimentally preferred, are addressed. Finally, a comparison with the corresponding Lewis acid mediated reactions with propene and propyne is made to compare the reactivity of the hetero-multiple bond with the one of a $\text{C}=\text{C}$ or $\text{C}\equiv\text{C}$ bond.

2. Computational details

MP2 and DFT calculations were carried out with the GAMESS (US)⁷ and GAUSSIAN⁸ programs respectively, and the results were visualised with MOLDEN⁹ or PLATON.¹⁰ Molecular geometries were fully optimized using the post-Hartree–Fock method MP2 and the DFT method B3LYP in combination with the basis set 6-31G*¹¹ for all atoms. All stationary points were characterised as local minima or transition states, according to their number of imaginary harmonic vibrational frequencies. For all transition states, the vibration associated with the imaginary frequency was examined for being consistent with the ring formation. Intrinsic reaction pathways were traced at MP2/6-31G* level of theory from the transition states towards both reactant and product direction along the imaginary vibrational mode using the algorithm developed by González and Schlegel.¹² All transition states correctly connect reactants and products. Single point calculations with higher level basis sets were performed on all stationary states (MP2/6-31++G**//MP2/6-31G*, MP2/6-311++G**//MP2/6-31G* and B3LYP/6-311++G**//B3LYP/6-31G*). The topological analysis of the charge density was performed with the program MORPHY.¹³ Critical points were located by using the eigenvector following method as implemented in the program.¹⁴ The respective wavefunction input files were generated by GAMESS (US) from single point calculations (MP2/6-31G*) on each individual IRC point. For selected molecular structures these calculations were repeated with wavefunctions from MP2/6-311++G**//MP2/6-31G*, B3LYP/6-31G**//B3LYP/6-31G* and B3LYP/6-311++G**//B3LYP/6-31G* calculations.

3. Results and discussion

Geometry optimisations at MP2/6-31G* and B3LYP/6-31G* levels of theory were performed for the reactants **1a–c**, **2a–c**, **5** and **10** and the products **4a–d**, **7**, **9**, **12** and **14**, whose structures are shown in Scheme 1. The transition states of all reactions were located. Their MP2-geometries are depicted in Figures 1 and 2, selected bond distances and angles are given in Table 1. Relative energies and dipole moments of the transition states and products are listed in Table 2, together with the relative energies of the Lewis acid free reactions published earlier.⁵



Scheme 1. Lewis acid mediated reactions of benzonitrile oxide with dipolarophiles **1**, **5** and **10**.

The structure of benzonitrile oxide **2a** is in good agreement with the solid state structure of closely related substituted benzonitrile oxides.¹⁵ The N–O bond distances calculated with MP2 or B3LYP are only 0.02–0.03 Å shorter and the C–N bond distances are 0.02–0.04 Å longer than the average experimental values. No experimental data is available on structures of Lewis acid coordinated nitrile oxides, although such species are postulated to exist in solution.¹⁶ Lewis acid complexes of nitriles, however, have been studied intensely

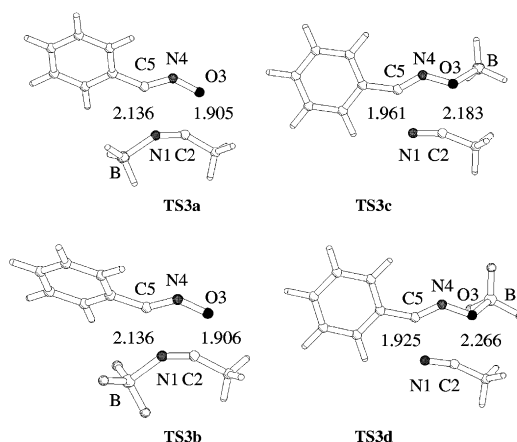


Figure 1. Transition states in the Lewis acid mediated reaction of benzonitrile oxide with acetonitrile.

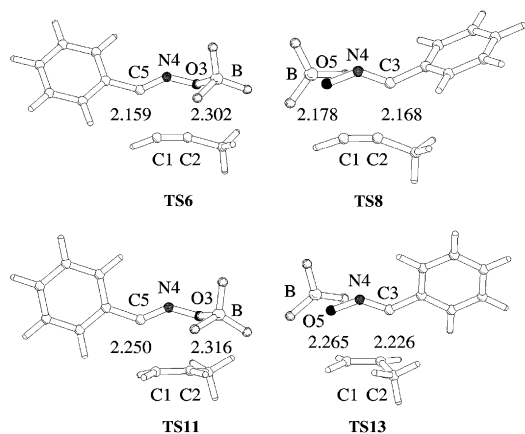


Figure 2. Transition states in the Lewis acid mediated reaction of benzonitrile oxide with propyne and propene.

with computational and experimental methods. The structure of MeCN-BF_3 **1b** in the gas phase,¹⁷ with a B–N distance of 2.011 Å and a N–B–F angle of 95.6°, differs substantially from the one found in the solid state,¹⁸ where a B–N distance of 1.630 Å and a N–B–F angle of 105.6° was observed. A recent computational study¹⁹ examined the structure and bonding of **1b** using a range of methods and basis sets to find two types of equilibrium structures, one with a B–N distance of 1.8–1.9 Å and another with 2.2–2.3 Å, and an extremely shallow potential energy profile along the B–N bond over the whole range of 1.8–2.4 Å. In our calculations, MP2 and B3LYP produced an energy minimum structure with a B–N distance of 1.88 and 1.90 Å, respectively. The acetonitrile complex with BH_3 is known to exist in the condensed phase but it dissociates in the gas phase.²⁰ This suggests an easily variable B–N distance as in the case of the BF_3 complex, and also that BH_3 acts

Table 1. Table of selected bond lengths (Å) and angles (degree) for MP2/6-31G* geometry optimised transition states **TS3a–d**, **TS6**, **TS8**, **TS11** and **TS13**

	TS3a	TS3b	TS3c	TS3d	TS6	TS8	TS11	TS13
1-2	1.201 (1.186)	1.200 (1.185)	1.200 (1.173)	1.196 (1.171)	1.243 (1.228)	1.245 (1.231)	1.370 (1.364)	1.375 (1.368)
2-3	1.905 (1.907)	1.906 (1.920)	2.183 (2.423)	2.266 (2.485)	2.302 (2.590)	2.168 (2.275)	2.316 (2.323)	2.226 (2.287)
3-4	1.255 (1.259)	1.250 (1.258)	1.286 (1.287)	1.297 (1.290)	1.247 (1.271)	1.237 (1.207)	1.253 (1.202)	1.237 (1.209)
4-5	1.228 (1.202)	1.225 (1.196)	1.220 (1.208)	1.219 (1.207)	1.226 (1.201)	1.240 (1.274)	1.230 (1.273)	1.249 (1.275)
5-1	2.136 (2.333)	2.136 (2.345)	1.961 (2.003)	1.925 (1.984)	2.159 (2.236)	2.178 (2.338)	2.250 (2.500)	2.265 (2.363)
X-B	1.631 (1.592)	1.696 (1.679)	1.698 (1.642)	1.671 (1.657)	1.905 (1.700)	2.186 (1.716)	1.814 (1.698)	1.920 (1.724)
1-2-3	109.9 (110.4)	108.6 (108.7)	102.2 (95.3)	96.9 (92.5)	99.7 (95.1)	103.0 (101.0)	99.8 (98.5)	101.7 (98.7)
2-3-4	99.5 (102.4)	99.5 (101.9)	93.8 (91.6)	92.7 (91.2)	95.4 (93.0)	98.3 (102.6)	97.6 (96.0)	99.8 (104.2)
3-4-5	135.6 (138.9)	136.8 (141.6)	133.0 (134.7)	132.4 (134.2)	138.7 (137.9)	137.0 (134.7)	139.3 (138.4)	138.3 (135.5)
4-5-1	93.3 (88.4)	92.0 (86.2)	102.5 (103.7)	104.2 (104.6)	98.1 (102.9)	96.5 (95.9)	98.7 (102.6)	97.4 (96.4)
5-1-2	101.6 (99.7)	103.1 (101.5)	108.4 (114.4)	111.9 (117.1)	108.1 (110.9)	105.3 (105.4)	104.3 (104.1)	102.3 (103.3)
1-2-Me	147.8 (149.6)	148.6 (150.5)	157.6 (169.8)	160.8 (171.6)	163.4 (175.7)	157.2 (155.1)	123.1 (125.2)	121.9 (123.0)
N-C-Ph	140.6 (151.0)	142.0 (153.2)	141.5 (143.5)	141.2 (143.3)	137.7 (145.4)	134.0 (143.9)	135.9 (144.5)	134.1 (142.5)
Y-X-B	146.3 (148.6)	141.4 (139.5)	113.2 (117.5)	111.7 (116.1)	111.1 (115.3)	107.9 (116.5)	112.0 (116.2)	111.3 (114.8)
X-B-(F/H)	104.6 (106.0)	103.7 (104.3)	102.4 (103.9)	103.2 (103.5)	98.7 (102.7)	95.1 (102.2)	100.2 (102.4)	98.5 (102.0)

The values for the B3LYP/6-31G* optimised geometries are given in parenthesis.

Table 2. Relative energies (kcal/mol) and dipole moments (Debye) for the BF_3 -mediated reactions of benzonitrile oxide **2** with acetonitrile **1**, propyne **5** and propene **10** (relative energy of dipolarophile+dipole=0 kcal/mol)

Method	MP2/6-31G*						B3LYP/6-31G*	
	Reactants		TS		Product		TS	Product
	μ	<i>E</i>	μ	<i>E</i>	μ	<i>E</i>	<i>E</i>	
1a+2a → 4a	2.8	+12.3 (+12.4)	3.8	−56.9 (−50.1)	2.5	+16.7 (+14.7)	−54.1 (−48.1)	
1b+2a → 4b	3.6	+6.4 (+12.4)	4.4	−61.8 (−50.1)	3.0	+9.0 (+14.7)	−60.8 (−48.1)	
1c+2b → 4c	5.6	+7.8 (+12.4)	6.1	−44.5 (−50.1)	3.3	+7.8 (+14.7)	−45.7 (−48.1)	
1c+2c → 4d	7.0	+6.3 (+12.4)	7.9	−48.2 (−50.1)	2.6	+6.8 (+14.7)	−49.4 (−48.1)	
5+2b → 7	9.5	+5.7 (+6.4)	7.8	−81.3 (−82.1)	4.4	+9.9 (+14.9)	−77.8 (−74.7)	
5+2b → 9	8.3	+7.3 (+8.6)	6.8	−77.9 (−79.1)	4.9	+14.2 (+18.5)	−72.9 (−69.7)	
10+2b → 12	9.4	+2.4 (+4.5)	8.2	−54.5 (−47.7)	8.1	+9.9 (+14.1)	−45.5 (−38.6)	
10+2b → 14	9.3	+3.8 (+5.0)	7.8	−51.1 (−45.1)	8.6	+13.3 (+17.1)	−41.1 (−34.5)	

Method	MP2/6-31+G**/MP2/6-31G*		MP2/6-311++G***/MP2/6-31G*		B3LYP/6-311++G***/B3LYP/6-31G*	
	TS	Product	TS	Product	TS	Product
	<i>E</i>	<i>E</i>	<i>E</i>	<i>E</i>	<i>E</i>	<i>E</i>
1a+2a → 4a	+11.1	−56.8	+12.3	−55.6	+20.2	−46.0
1b+2a → 4b	+4.3	−61.9	+7.5	−58.2	+13.1	−50.3
1c+2b → 4c	+6.1	−44.8	+7.4	−42.1	+11.0	−38.2
1c+2c → 4d	+4.3	−47.1	+6.4	−45.9	+8.9	−41.6
5+2b → 7	+4.3	−80.0	+5.4	−77.8	+12.9	−68.0
5+2b → 9	+6.4	−76.8	+7.0	−75.0	+17.3	−63.4
10+2b → 12	+1.4	−54.2	+1.8	−51.9	+11.8	−38.6
10+2b → 14	+2.8	−51.6	+2.8	−49.7	+15.2	−34.8

The relative energies of the corresponding Lewis acid free reactions⁵ are given in parenthesis.

a weaker Lewis acid than BF_3 . The latter is confirmed from the experimental heats of formation,²¹ the vibrational frequencies and force constants of the B–N bond.^{20,22} Our calculations provided structures with a rather short B–N distance of 1.59 Å (MP2) and 1.55 Å (B3LYP), in agreement with other theoretical studies.²⁰

3.1. BF_3 -mediated reaction of benzonitrile oxide with acetonitrile

This section summarises the results obtained with MP2/6-31G* and discusses the effects of a strong Lewis acid, modelled by BF_3 . When coordinated to the nitrile as in reaction $\mathbf{1b} + \mathbf{2a} \rightarrow \mathbf{4b}$, the activation barrier for the cycloaddition to benzonitrile oxide is 6.0 kcal/mol lower than in the Lewis acid free reaction.⁵ This shows that Lewis acids are indeed able to activate nitriles towards cycloadditions with nitrile oxides. The BF_3 -coordinated product $\mathbf{4b}$ is more stable than the Lewis acid free product, and the thermodynamic driving force of the reaction is increased by 11.7 kcal/mol. BF_3 coordination to the nitrile favours the reaction both kinetically and thermodynamically.

The intrinsic reaction path (Fig. 3 left) shows more details about the reaction mechanism. Most prominently, a trend towards a sequential bond formation is observed. The $\text{C}\cdots\text{O}$ bond is established at an earlier stage than the $\text{C}\cdots\text{N}$ bond, indicating that the reaction, although still concerted, tends towards a nucleophilic attack of the oxygen atom of the nitrile oxide at the nitrile carbon. This suggests that the reaction is driven by an interaction of an unoccupied orbital of the nitrile with an occupied one of the nitrile oxide. In the Lewis acid free reaction, the sequence of bond formation and the orbital involvement was inverted.⁵ Coordination of a strong Lewis acid to the nitrile thus switches the mechanism

from an ‘inverse electron demand’ to a ‘normal electron demand’ cycloaddition, as postulated in our hypothesis.

The geometric changes along the intrinsic reaction path also help to understand the activation mechanism in more detail. In the initial phase of the reaction, the reactants approximate each other and the formerly linear B–N≡C–C unit bends to adopt angles of 148.6 (N=C–C) and 141.4 (C=N–B) in the transition state. A shortening of the B–N bond during this process suggests that the interaction of the Lewis acid with the nitrile becomes stronger. As long as the Lewis acid complex with the nitrile is linear, coordination takes place through the sp hybridised nitrogen lone pair orthogonal to the orbitals involved in the cycloaddition, where the Lewis acid has relatively little influence on the FMO energies and the charge distribution within the nitrile. The bending of the Lewis acid nitrile complex requires a re-hybridisation of the $\text{C}\equiv\text{N}$ bond to an sp^2 nitrogen and carbon. As a consequence, one of the former π -bonds of the $\text{C}\equiv\text{N}$ breaks open.

The transition state is of an early character, as frequently observed for 1,3-dipolar cycloadditions,^{4,5,23} and the ring formation and the transformations of the two $\text{C}\equiv\text{N}$ bonds into $\text{C}=\text{N}$ bonds occur after the transition state only. This process is accompanied by a weakening of the N–B bond until the Lewis acid is almost released from the molecule. The N–B distance is longest at the point of the intrinsic reaction path at which the ring can be considered formed as no further changes in the bond distances within the ring take place (stride 5.5). From this point on, the heterocycle re-coordinates to the Lewis acid and this process is exothermic. The N–B bond in the final complex is slightly shorter and stronger than in the complex with the nitrile, suggesting that an exchange of product by reactant will be inefficient. The reaction is not catalytic but Lewis acid mediated.

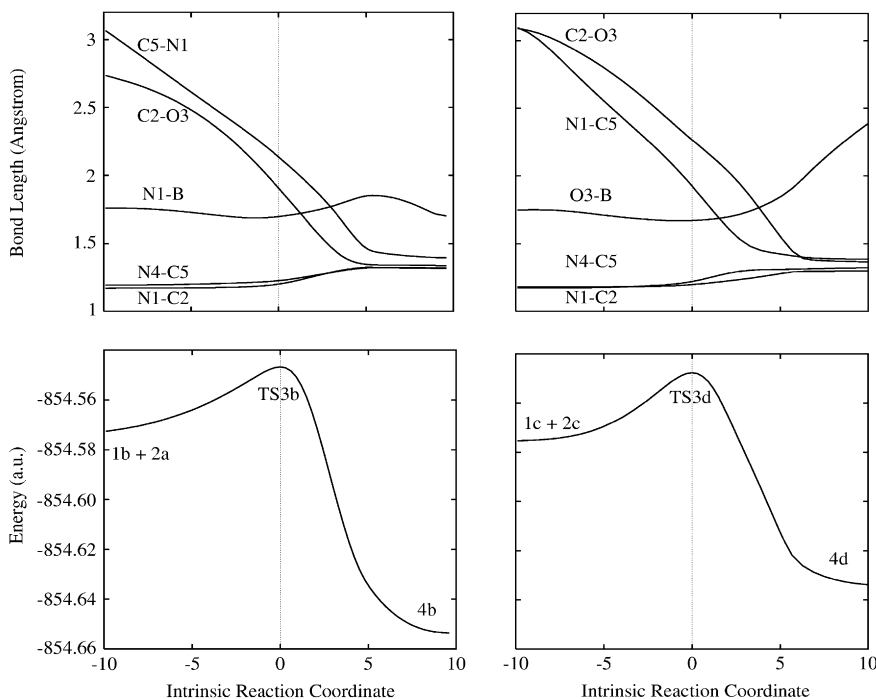


Figure 3. Intrinsic reaction coordinates ($\text{amu}^{1/2} \text{ bohr}$) for the reactions $\mathbf{1b} + \mathbf{2a} \rightarrow \mathbf{4b}$ (left) and $\mathbf{1c} + \mathbf{2c} \rightarrow \mathbf{4d}$ (right).

For the alternative reaction in which the BF_3 coordinates to the oxygen atom of the nitrile oxide rather than to the nitrile ($\mathbf{1c} + \mathbf{2c} \rightarrow \mathbf{4d}$), the activation barrier is equally lowered with respect to the Lewis acid free reaction, approximately to the same extent as for the reaction of Lewis acid-coordinated acetonitrile ($\mathbf{1b}$) with benzonitrile oxide ($\mathbf{2a}$) described above. BF_3 thus promotes the reaction, independent of its coordination site. Interestingly, however, the product does not receive additional stabilisation by coordination, and its relative energy is practically the same as for the Lewis acid free reaction. Coordination of BF_3 to the nitrile oxide favours the cycloaddition only kinetically, but not thermodynamically.

The intrinsic reaction path (Fig. 3 right) shows that the N–C bond is formed at an earlier stage than the C–O bond. The order of bond formation, and with this the orbital interaction, switches depending on the coordination site of the Lewis acid. The cycloaddition of nitriles with nitrile oxides is therefore best described as a Sustmann type II cycloaddition,²⁴ as initially postulated.

The interaction of the Lewis acid with the nitrile oxide becomes stronger along the reaction coordinate towards the transition state, just as in the reaction where the Lewis acid was coordinated to the nitrile. However, starting from the point where the ring closure and bond reorganisation takes place, the B–O bond weakens continuously and BF_3 is eventually released from the heterocycle. By the end of the reaction, the BF_3 moiety is 2.4 Å away from the oxygen. The interaction of BF_3 with the reactant is stronger than with the product, and the reaction is expected to be catalytic.

To check the validity of the computational method, all calculations were repeated with higher level basis sets and also with the commonly used DFT method B3LYP. As shown in Table 2, the computational method and the basis set used have little influence on the energy profiles of the two reactions. MP2 single point calculations using the higher level basis sets 6-31+G* and 6-311++G** gave the same trends as with MP2/6-31G*, and the relative energies of the products and the activation barriers are similar or only marginally lower. Also the DFT method B3LYP in combination with the 6-31G* basis set reproduces the MP2 calculations quite closely. The activation energies are slightly higher and in agreement with the known fact that MP2 generally tends to underestimate activation barriers. The B3LYP/6-31G* optimised transition states are earlier in character and the bond formation is slightly less advanced than in the MP2 optimised structures. B3LYP is far more vulnerable to effects of the basis set than MP2, and the reaction energies obtained from single point calculations using 6-311++G** are 8–10 kcal/mol lower and the activation barriers 2–4 kcal/mol higher than with 6-31G*.

3.2. Topological analysis of the charge density using the theory of ‘atoms in molecules’

Bond distances are affected by a number of factors (e.g., ring strain or steric interactions) and may not accurately reflect bond orders. In order to confirm the discussion above we decided to look at the charge density in the bond, as a more reliable measure for the bond strength, by using the

theory of ‘Atoms in Molecules’ (AIM), introduced by Bader.²⁵ A bond is characterised by: (a) the charge density at the critical point ρ_b as a measure of how much charge is accumulated between the bonded nuclei. Generally, ρ_b can be correlated with the bond order and reflects the strength of a bond. (b) The Laplacian $\nabla^2\rho_b$ as a measure of local charge concentration ($\nabla^2\rho_b < 0$) or local charge depletion ($\nabla^2\rho_b > 0$). (c) The ellipticity as a measure for the π character of a bond but also of its structural stability. In a strict sense, for atoms to be bonded there must be an atomic interaction line connecting the atoms through a BCP, and there cannot be any forces so the system needs to be in a stationary state for this to be valid. Nevertheless, the AIM concept has been applied to non-stationary states along an IRC in a topological analysis of $\text{S}_{\text{N}}2$ reactions of methyl halides,²⁶ although the authors considered changes of atomic properties rather than changes at the BCP. In another example, the properties of bond critical points along the IRC have been used to establish a quantitative structure–property relationship in calculated reaction pathways.²⁷ In a similar sense, we now analysed the two reactions $\text{MeCN} + \text{BF}_3 + \text{PhCNO}$ and $\text{PhCNO} + \text{BF}_3 + \text{MeCN}$ with respect to changes of bond properties along the IRC. The results are shown in Table 3 and Figures 4 and 5.

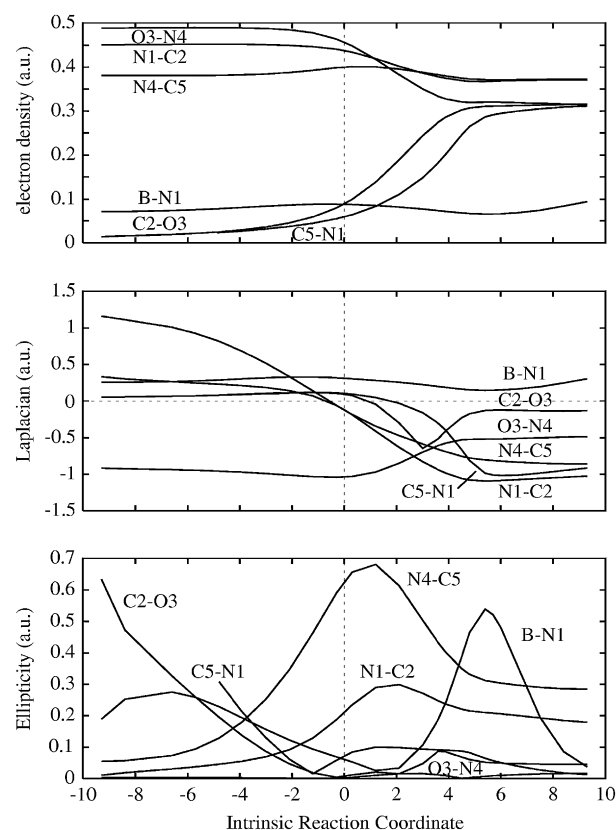
First, the bond characteristics in the reactants and products, obtained from MP2/6-31G* wavefunctions, are discussed. Charge densities obtained from MP2/6-311++G** or B3LYP/6-31G* or B3LYP/6-311++G** wavefunctions are numerically very similar, as shown in Table 3. The charge density at the BCP of the $\text{C}\equiv\text{N}$ bonds is $\rho_b = 0.45$ a.u. for the nitrile $\mathbf{1c}$, and $\rho_b = 0.38$ a.u. for the nitrile oxide $\mathbf{2a}$. These comparatively high values are typical for triple bonds and compare well with literature values (e.g., $\rho_b = 0.4912$ a.u. for aliphatic nitriles, determined from the RHF/6-31++G**//RHF/6-31G** wavefunctions,²⁸ or $\rho_b = 0.475$ a.u. for acetonitrile (RHF/4-31G**),²⁹ or $\rho_b = 0.5069$ a.u. for $\text{C}\equiv\text{O}$, calculated from the RHF/6-311++G**//RHF/6-311++G** wavefunction).²⁵ The charge density of the nitrile oxide is lower, reflecting its two resonance structures, one of which has double bond character ($\text{R}-\text{C}\equiv\text{N}^+-\text{O}^- \leftrightarrow \text{R}-\text{C}^-=\text{N}^+=\text{O}$). BF_3 -coordination has little effect on the charge density of the nitrile and ρ_b is reduced by less than 0.001 a.u. The nitrile oxide responds more strongly to the presence of the Lewis acid and ρ_b in the C–N bond is increased by 0.014 a.u. The Laplacian for $\text{C}\equiv\text{N}$ bonds is positive, in contrast to other covalent bonds for which negative values for $\nabla^2\rho_b$ are observed. It varies in an order of +0.19 a.u. for nitrile, +0.33 a.u. for coordinated nitrile, and +1.16 a.u. for the free or coordinated nitrile oxide. These values are consistent with literature data (+0.568 a.u. for MeCN ²¹ and +0.9796 a.u. for CO).²⁵ The ellipticity is small (0.001–0.05 a.u.), in agreement with a cylindrical electron distribution around the triple bond. The charge density in the $\text{C}=\text{N}$ bonds in the oxadiazoles $\mathbf{4b}$ and $\mathbf{4d}$ is in a range of 0.37–0.39 a.u. and compatible with values reported for other double bonds ($\text{C}=\text{C}$ of ethene: 0.3627 a.u.; $\text{C}=\text{O}$ of formaldehyde: 0.4308 a.u.).²⁵ The Laplacian for $\text{C}=\text{N}$ bonds is strongly negative (–0.8 to –1.1 a.u.) and similar to the one of ethene (–1.1892 a.u.).²⁵ The ellipticity is comparatively large (0.18–0.28), accounting for the presence of one π -bond. For single bonds, the charge density at the BCP is typically 0.29–0.32 a.u., with exception of the

Table 3. Charge densities ρ_b (a.u.) of selected bond critical points (reactions **1b+2a**→**4b** and **1c+2c**→**4d**)

Compound	Bond	MP2/ 6-31G*	MP2/6- 311++G** //MP2/ 6-31G*	B3LYP/ 6-31G*	B3LYP/6- 311++G** //B3LYP/ 6-31G*
Reaction 1b+2a → 4b					
1b	N1≡C2	0.45185	0.45609	0.46417	0.47201
	N1–B	0.06261	0.06298	0.06106	0.06290
2a	N4≡C5	0.38039	0.38222	0.40121	0.40655
	N4–O3	0.49721	0.50491	0.48727	0.48942
TS3b	N1=C2	0.43747	0.43810	0.44536	0.44943
	C2⋯O3	0.08904	0.08885	0.08488	0.08377
	O3–N4	0.45646	0.46340	0.44277	0.44356
	N4=C5	0.39982	0.39819	0.40878	0.41134
	C5⋯N1	0.05931	0.05989	0.03878	0.03893
4b	N1–B	0.08831	0.08855	0.10054	0.10169
	N1=C2	0.37251	0.36690	0.36579	0.36929
	C2–O3	0.31581	0.31240	0.32020	0.31825
	O3–N4	0.31315	0.31835	0.30262	0.30316
	N4=C5	0.37260	0.36740	0.37356	0.36929
	C5–N1	0.31427	0.30907	0.30627	0.30052
	N1–B	0.09634	0.09657	0.10270	0.10375
Reaction 1c+2c → 4d					
1c	N1≡C2	0.45202	0.45686	0.46506	0.47470
2c	N4≡C5	0.39407	0.39635	0.41041	0.41614
	N4–O3	0.47200	0.47800	0.46671	0.46780
	O3–B	0.04314	0.04525	0.03996	0.04136
TS3d	N1=C2	0.44429	0.44660	0.45648	0.46391
	C2⋯O3	0.03896	0.03825	0.02562	0.02522
	O3–N4	0.41368	0.41927	0.40860	0.40879
	N4=C5	0.41755	0.41629	0.41123	0.41290
	C5⋯N1	0.08332	0.08467	0.07522	0.07513
	O3–B	0.08513	0.08565	0.09540	0.09678
4d	N1=C2	0.38900	0.38395	0.38465	0.38008
	C2–O3	0.29049	0.28724	0.29749	0.29498
	O3–N4	0.31343	0.31799	0.30217	0.30218
	N4=C5	0.36849	0.36377	0.36911	0.36491
	C5–N1	0.32880	0.32365	0.32007	0.31461
	O3–B	(no BCP)	(no BCP)	0.01571	0.01564

O3–N4 bond of the nitrile oxide ($\rho_b=0.49$ a.u. for uncoordinated species **2a** and $\rho_b=0.45$ a.u. for the BF₃-coordinated **2c**). This again can be attributed to the relevance of a resonance structure with N=O bond character (R–C≡N⁺–O[−] ↔ R–C[−]=N⁺=O). The Laplacian is moderately negative and in an order of −0.12 a.u. for C2–O3, −0.46 to −0.48 a.u. for O3–N4, and −0.9 to −1.2 a.u. for C5–N1 bonds. The ellipticity is small, as expected for a σ -bond (0.002–0.07 a.u.). The bond characteristics of the Lewis acid–Lewis base bond indicate a closed shell interaction. This can be seen in the small value of the charge density at the BCP (0.04–0.09 a.u. for the B–N or B–O bonds in **1b**, **2c** and **4b**) and a positive value for $\nabla^2\rho_b$ (0.23–0.30 a.u.). The ellipticity is very variable and spreads from 0.25 in the BF₃-coordinated nitrile **1b**, to 0.06 in the nitrile oxide–BF₃ complex **2c**, and 0.03 for the oxadiazoline–BF₃ complex **4b**. The ellipticity is often associated with bond stability, and it would appear that the oxadiazoline forms a stable complex with BF₃ on the basis of the combination of a low ε value and a relatively high ρ_b . This agrees well with energy considerations discussed in the previous section.

Along the IRC of a reaction, bond formation is reflected in an increase of electron density at the BCP. A bond breakage can be inferred by extremely low values of ρ_b or complete disappearance of the BCP, and an increase of ε indicating bond instability. Changes in bond order can be observed in

**Figure 4.** Properties of selected BCP along the IRC of reaction **1b+2a**→**4b**. Top: charge density ρ_b ; middle: Laplacian $\nabla^2\rho_b$; bottom: ellipticity ε . All quantities are given in atomic units.

changes of ρ_b , $\nabla^2\rho_b$ and ε passing a characteristic maximum. For the reaction with the BF₃-coordinated nitrile (**1b+2a**→**4b**), these changes are shown in Figure 4. All bond formations and bond rearrangements take place after the transition state, at a stride of 0–5, confirming the early character of the transition state. The accumulation of charge density in the C2–O3 bond is slightly advanced and accompanied by a reduction of charge in the O3–N4 bond. The subsequent accumulation of charge in the C5–N1 bond seems to go in parallel with charge depletion in the N1–C2 bond. This suggests that the cycloaddition occurs by an electron transfer from the oxygen of the nitrile oxide onto the nitrile carbon, and then from the nitrile nitrogen onto C5 of the nitrile oxide. In the transition state **TS3b**, the C2⋯O3 bond has accumulated a charge density of 0.09 a.u. (28% of its final value in the product **4b**), whereas ρ_b in the C5⋯N1 bond is 0.06 a.u. (19% of its final value) only. Concomitantly, ρ_b in the O3–N4 bond has decreased by 0.04 a.u., as compared to the starting material, whereas the corresponding decrease of ρ_b in the N1–C2 bond is only 0.014 a.u. Also the bonding of the Lewis acid in the course of the reactions is worth noting. When coordinated to the N1 atom, the charge density between N1 and B increases on the way to the transition state and decreases after it. At about stride 5 to 6, the charge density is lowest and the ellipticity has a maximum, indicating an instability at which the Lewis acid is nearly released from the newly formed heterocycle. However, both ρ_b and ε indicate that the Lewis acid re-coordinates to form a stable complex towards the end of the reaction. When the Lewis acid is coordinated to the nitrile oxide, as in reaction

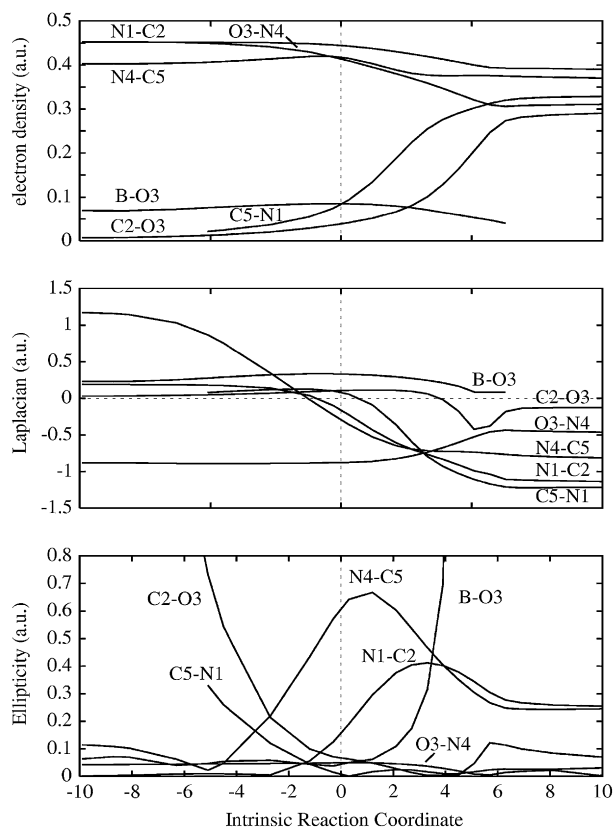


Figure 5. Properties of selected BCP along the IRC of reaction **1c+2c** → **4d**. Top: charge density ρ_b ; middle: Laplacian $\nabla^2\rho_b$; bottom: ellipticity ε . All quantities are given in atomic units.

1c+2c → **4d**, the reaction profile is significantly different, as shown in Figure 5. Although the bond formations and bond rearrangements also take place after the transition state, the sequence of bond formation is inverted and the electron flow is in the opposite direction. In the transition state **TS3d**, the charge density in the C5···N1 bond is accumulated to 0.08 a.u. (25% of its final value in the product **4d**), but ρ_b in the C2···O3 bond is only 0.04 a.u. (13% of its final value). It appears that the charge builds up in the newly formed C5–N1 bond when the O3–N4–C5 moiety of the nitrile oxide is most affected. Subsequently, the formation of the C2–O3 bond goes in parallel with a depletion of charge in the N1–C2 bond. The bond between the B atom of the Lewis acid and O3 of the nitrile oxide shows an initial increase in charge density along the IRC and the bond is strongest in the TS. After the TS it is continuously weakened and eventually broken. This can be seen in the drastic increase of ε along stride 2–7 and the disappearance of the bond critical point at stride 7. In summary, the results derived from the topological analysis of the electron density confirm what the changes of geometrical parameters along the IRC suggested.

3.3. BH₃-mediated reaction of benzonitrile oxide with acetonitrile

In the following section, the effect of a weak Lewis acid BH₃ on the reactivity and reaction mechanism is assessed. As for the BF₃-mediated reaction, the computational method (MP2 or B3LYP) and the basis set used (6-31G*, 6-31+G* and

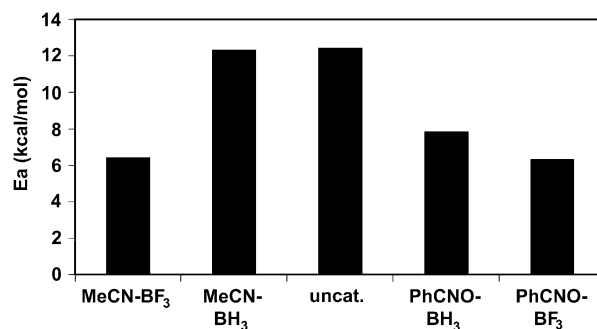


Figure 6. Activation energies (kcal/mol) for the uncatalysed reaction of benzonitrile oxide with acetonitrile, and the Lewis acid mediated reactions (A) and (B) using BF₃ or BH₃ as Lewis acids.

6-311++G**) give comparable results. Coordination of BH₃ to the oxygen atom of benzonitrile oxide (reaction **1c+2b** → **4c**) also results in a lower activation energy, compared to the Lewis acid free reaction. As expected, the effect of BH₃ is smaller than that of BF₃. The relative energy of the product is comparable to that obtained from the Lewis acid free reaction, thus the thermodynamics remain essentially unchanged. The IRC of the reaction suggests the same sequence of bond formation and orbital interaction as in the reaction with BF₃ as a Lewis acid. A release of the Lewis acid is observed towards the end of the reaction so the reaction should be catalytic, as in the case of the BF₃ promoted reaction.

If BH₃ is bound to the nitrile, the intrinsic reaction path resembles that of the reaction of the nitrile–BF₃ complex, with the C···O bond forming slightly earlier than the C···N bond. This suggests that the relevant orbital interaction is switched already and the reaction is of ‘normal electron demand’. The Lewis acid is trapped by coordination to the product in the final stage of the reaction, leading to a thermodynamic stabilisation of the product. However, in contrast to BF₃, BH₃ is too weak a Lewis acid to promote the reaction kinetically. Its activation barrier is practically the same or even slightly higher than for the uncatalysed reaction (MP2: 12.3 kcal/mol vs 12.6 kcal/mol;⁵ B3LYP: 16.7 kcal/mol vs 14.7 kcal/mol;⁵ see also Fig. 6).

3.4. Which is the preferred binding site of the Lewis acid?

Under experimental conditions, a preferred binding of the Lewis acid to one of the substrates will decide, which activation pathway is more relevant and thus determines the outcome of the reaction. Depending on the computational method and basis set used, the relatively weak and soft Lewis acid BH₃ is 8.7–11.2 kcal/mol more stabilised when coordinated to the nitrile (E(**1a**)+E(**2a**)-E(**1c**)-E(**2b**)). This is also reflected in the bond distances to the substrate. The B···N bond in **1a** is significantly shorter than the B···O bond in **2b** (MP2: 1.595 Å vs 1.770 Å). As a consequence, BH₃ will bind to the functional group which it is unable to activate. A weak and soft Lewis acid is not expected to promote the reaction to a significant extent.

In the case of BF₃ as a stronger and harder Lewis acid, both MeCN+nitrile oxide BF₃ adduct, or MeCN–BF₃+nitrile

oxide are similar in energy, the O-adduct being 0.5 kcal/mol more stable than the N-adduct (MP2/6-31G*). With the other computational methods the order of stability can be inverted but the energy difference remains in a range 0.05–1.1 kcal/mol. Both pathways are expected to play a role under experimental conditions. Since both coordination modes lead to a decrease of the activation energy, the overall reaction will be promoted. However, the N-coordinated product **4b** is significantly more stable than the O-coordinated **4d** ($\Delta E=13.1$ kcal/mol (MP2) and 11.4 kcal/mol (B3LYP)). As a result, the reaction will not be catalytic but product inhibited, because the Lewis acid that is released from the oxygen atom in the course of the reaction of the coordinated nitrile oxide will be trapped by coordination to the nitrogen of the product in an exothermic reaction.

Overall, which coordination mode is preferred appears to depend strongly on the individual Lewis acid. To achieve a catalytic reaction, a hard Lewis acid with little tendency to coordinate to nitrogen seems most promising.

3.5. BF₃-mediated reaction of benzonitrile oxide with propyne or propene

To answer the question as to whether Lewis acids promote the cycloaddition of benzonitrile oxide with other dipolarophiles in a similar way, the reactions of the BF₃ adduct of benzonitrile oxide with propyne and propene were studied. In the reactions with propyne ((C) in Scheme 1) practically the same amount of energy is released as in the non-catalysed case (81.3 vs 82.1 kcal/mol, and 77.9 vs 79.1 kcal/mol for the regioisomeric products **7** and **9**). The Lewis acid does not change the thermodynamics of the reaction. The activation energy of both reactions is only marginally lower than in the non-catalysed case (5.7 vs 6.4 kcal/mol, and 7.9 vs 8.3 kcal/mol). With B3LYP the differences are a bit larger, indicating that the Lewis acid tends to activate, although the effect may be weak. The regiochemistry is unaltered by the Lewis acid, both thermodynamic and kinetic arguments are in favour of the 3,5-disubstituted isomer as preferred product. The intrinsic reaction paths (Figs. S2 and S3 of the Supplementary data) show that both energy profile and the change of characteristic distances are very similar to the uncoordinated reaction described in our previous publication,⁵ with respect to concertedness and an almost synchronous bond formation. The new element is the behaviour of the BF₃, which is released in the course of the reaction. For this reason the reaction could be promising for Lewis acid catalysis. However, the activating effect of the Lewis acid may be too weak to be of practical use. With this in mind, it is not surprising that no experimental report on Lewis acid promoted cycloaddition of nitrile oxides to alkynes exists in the literature.

The reaction of nitrile oxides with appropriate alkenes, in contrast, can be promoted in the presence of appropriate Lewis acids. Magnesium ions are most suitable,³⁰ but also nickel complexes,³¹ zinc salts³² or lanthanide triflates were used.^{33,30g} Our calculations of the reaction of BF₃-coordinated benzonitrile oxide with propene ((D) in Scheme 1) showed that both regioisomeric products are slightly stabilised by the Lewis acid (–54.5 vs –47.7 kcal/mol, and –51.1 vs –45.1 kcal/mol with MP2; –38.6 kcal/mol, and

–41.1 vs –34.5 kcal/mol with B3LYP). The activation barriers are somewhat lowered for both regioisomeric pathways (approx. 2 kcal/mol with MP2 and 4 kcal/mol with B3LYP). Overall, the reaction is weakly promoted by the Lewis acid. The regioselectivity of the reaction remains unchanged in the presence of the Lewis acid. As in the uncatalysed reaction, the 3,5-disubstituted regioisomer is both thermodynamically and kinetically preferred. The intrinsic reaction paths (Figs. S3 and S4 of the Supplementary data) show that the bond distance between the Lewis acid and the nitrile oxide slightly oscillates along the reaction coordinate, to eventually reform under stabilisation of the product. Whether the reaction is catalytic or not cannot be decided easily. The B···O bond distances in the nitrile oxide or the products are very similar, so that a ligand exchange with the reactant seems possible. Also a change of the Lewis acid, substrate or solvent effects may alter the situation. The possibility to coordinate both substrates to the same Lewis acid could be used to enhance the activating effect because the reaction becomes pseudo-intramolecular. This strategy has been used in a computational study of a magnesium-controlled cycloaddition of nitrile oxides and allylic alcohols.³⁴

The influence of the computational method and the basis set on the reaction of benzonitrile oxide with propyne and propene was analysed and showed some interesting results. As for the reaction with acetonitrile, MP2 gives consistent results. The dependence on the basis set (6-31G*, 6-31+G* or 6-311++G**) is small, with a variation of the relative energy values within a range of 1–3 kcal/mol. B3LYP, in contrast, seems not to perform overly well. Although the trends within a given dipole/dipolarophile combination are correctly reproduced, the comparison between different dipolarophiles gives inconsistent results: (i) the experimentally observed reactivity scale alkene>alkyne>nitrile of the Lewis acid free reaction is reproduced with MP2. B3LYP, however, predicts essentially the same activation barriers for all three reactions. (ii) For the Lewis acid mediated reactions, the relative energies calculated with MP2 or B3LYP differ quite significantly and show a trend nitrile>alkyne>alkene. Thus, the differences in reaction energies are in an order 1–2.5 kcal/mol for the nitrile, 3.5–5 kcal/mol for the alkyne and 9–10 kcal/mol for the alkene. The activation barriers differ by 0–4.5 kcal/mol, 5–6 kcal/mol and 8.5–9.6 kcal/mol, respectively. (iii) The basis set dependence is quite significant with B3LYP, but the differences are at least consistent for all reactions studied. When 6-311++G** is used in place of 6-31G* the products are predicted 10 kcal/mol and transition states 3 kcal/mol less stable. Overall, MP2 seems to outperform B3LYP when the reactivity of dienophiles with different functional groups is compared.

4. Conclusion

We have shown with the help of quantum mechanical calculations and an analysis of the topology of the charge density of relevant bonds along the IRC that the reaction of nitrile oxides and nitriles is a promising candidate for Lewis acid activation. The activation can occur via two different mechanisms: If the Lewis acid is coordinated to the nitrile oxide,

the reactant is activated and the product is easily released from the Lewis acid. Mechanistically, the cycloaddition is of ‘inverse electron demand’. If the Lewis acid is coordinated to the nitrile and strong enough, a reversal of the electronic requirements takes place and the cycloaddition is now dominated by an interaction of an occupied orbital of the dipolarophile with an unoccupied one of the dipole. The activating effect is not so much due to activation of the reactant but rather to a stabilisation of the transition state and product. As a result, formation of a stable complex of the product with the Lewis acid is expected.

Although the cycloaddition of nitrile oxide with nitrile or alkyne is mechanistically similar,⁵ the influence of a Lewis acid on these two reactions is entirely different. Compared to the large kinetic and thermodynamic effects predicted for the reaction with nitriles, the cycloaddition of nitrile oxides to alkynes is surprisingly insensitive to Lewis acids. Alkenes adopt an intermediate position and a weak activation is expected.

Acknowledgements

The authors thank the Department of Chemistry of the University of Surrey for support. Computational resources on a COMPAQ ES40 multiprocessor cluster (Columbus) at the Rutherford Appleton Laboratory (RAL), provided by the EPSRC National Service for Computational Chemistry Software are acknowledged.

Supplementary data

Electronic supplementary material containing intrinsic reaction coordinates for the reactions $5+2c \rightarrow 7$, $5+2c \rightarrow 9$, $10+2c \rightarrow 12$ and $10+2c \rightarrow 14$ may be accessed free of charge from the Tetrahedron website. Supplementary data associated with this article can be found in the online version, at doi:10.1016/j.tet.2007.03.169.

References and notes

- (a) Huisgen, R. *Angew. Chem., Int. Ed. Engl.* **1963**, *2*, 565–598; (b) Huisgen, R. *Angew. Chem., Int. Ed. Engl.* **1963**, *2*, 633–645; (c) *1,3 Dipolar Cycloaddition Chemistry*; Padwa, A., Ed.; Wiley-Interscience: New York, NY, 1984; Vols. 1–2; (d) Gothelf, K. V.; Jørgensen, K. A. *Chem. Rev.* **1998**, *98*, 863–909; (e) Gothelf, K. V.; Jørgensen, K. A. *Chem. Commun.* **2000**, 1449–1458.
- (a) Herbst, R. M.; Wilson, K. R. *J. Org. Chem.* **1957**, *22*, 1142–1145; (b) Demko, Z. P.; Sharpless, K. B. *Org. Lett.* **2001**, *3*, 4091–4094; (c) Fischer, B.; Hassner, A. *J. Org. Chem.* **1990**, *55*, 5225–5229; (d) Huisgen, R.; Sturm, H. J.; Binsch, G. *Chem. Ber.* **1964**, *97*, 2864–2867; (e) Armstrong, R. K. *J. Org. Chem.* **1966**, *31*, 618; (f) Doyle, M. P.; Buhro, W. E.; Davidson, J. G.; Elliott, R. C.; Hoekstra, J. W.; Oppenhuizen, M. J. *J. Org. Chem.* **1980**, *45*, 3657–3664; (g) Samuilov, Ya. D.; Solov'eva, S. E.; Kononov, A. I. *Dokl. Akad. Nauk. SSSR Ser. Khim.* **1980**, *255*, 606–609; (h) Padwa, A.; Kline, D. N.; Koehler, K. F.; Matzinger, M.; Venkatramanan, M. K. *J. Org. Chem.* **1987**, *52*, 3909–3917.
- (a) Wagner, G.; Pombeiro, A. J. L.; Kukushkin, V. Yu. *J. Am. Chem. Soc.* **2000**, *122*, 3106–3111; (b) Wagner, G.; Haukka, M.; Fraústo da Silva, J. J. R.; Pombeiro, A. J. L.; Kukushkin, V. Yu. *Inorg. Chem.* **2001**, *40*, 264–271; (c) Wagner, G.; Haukka, M. *J. Chem. Soc., Dalton Trans.* **2001**, 2690–2697; (d) Desai, B.; Danks, T. N.; Wagner, G. *Dalton Trans.* **2003**, 2544–2549; (e) Desai, B.; Danks, T. N.; Wagner, G. *Dalton Trans.* **2004**, 166–171; (f) Wagner, G. *Inorg. Chim. Acta* **2004**, *357*, 1320–1324.
- Wagner, G. *Chem.—Eur. J.* **2003**, *9*, 1503–1510.
- Vullo, V.; Danks, T. N.; Wagner, G. *Eur. J. Org. Chem.* **2004**, 2046–2052.
- (a) Leandri, G.; Palotti, M. *Ann. Chim.* **1957**, *47*, 376; (b) Huisgen, R.; Mack, W.; Anneser, E. *Tetrahedron Lett.* **1961**, 587–589.
- Schmidt, M. W.; Baldrige, K. K.; Boatz, J. A.; Elbert, S. T.; Gordon, M. S.; Jensen, J. H.; Koseki, S.; Matsunaga, N.; Nguyen, K. A.; Su, S. J.; Windus, T. L.; Dupuis, M.; Montgomery, J. A. *J. Comput. Chem.* **1993**, *14*, 1347–1363.
- Frisch, M. J.; Trucks, G. W.; Schlegel, H. B.; Scuseria, G. E.; Robb, M. A.; Cheeseman, J. R.; Montgomery, J. A., Jr.; Vreven, T.; Kudin, K. N.; Burant, J. C.; Millam, J. M.; Iyengar, S. S.; Tomasi, J.; Barone, V.; Mennucci, B.; Cossi, M.; Scalmani, G.; Rega, N.; Petersson, G. A.; Nakatsuji, H.; Hada, M.; Ehara, M.; Toyota, K.; Fukuda, R.; Hasegawa, J.; Ishida, M.; Nakajima, T.; Honda, Y.; Kitao, O.; Nakai, H.; Klene, M.; Li, X.; Knox, J. E.; Hratchian, H. P.; Cross, J. B.; Bakken, V.; Adamo, C.; Jaramillo, J.; Gomperts, R.; Stratmann, R. E.; Yazyev, O.; Austin, A. J.; Cammi, R.; Pomelli, C.; Ochterski, J. W.; Ayala, P. Y.; Morokuma, K.; Voth, G. A.; Salvador, P.; Dannenberg, J. J.; Zakrzewski, V. G.; Dapprich, S.; Daniels, A. D.; Strain, M. C.; Farkas, O.; Malick, D. K.; Rabuck, A. D.; Raghavachari, K.; Foresman, J. B.; Ortiz, J. V.; Cui, Q.; Baboul, A. G.; Clifford, S.; Cioslowski, J.; Stefanov, B. B.; Liu, G.; Liashenko, A.; Piskorz, P.; Komaromi, I.; Martin, R. L.; Fox, D. J.; Keith, T.; Al-Laham, M. A.; Peng, C. Y.; Nanayakkara, A.; Challacombe, M.; Gill, P. M. W.; Johnson, B.; Chen, W.; Wong, M. W.; Gonzalez, C.; Pople, J. A. *Gaussian 03, Revision C.01*; Gaussian: Wallingford, CT, 2004.
- Schaftenaar, G.; Noordik, J. H. *J. Comput.-Aided Mol. Des.* **2000**, *14*, 123–134.
- Spek, A.L. <http://www.cryst.chem.uu.nl/platon/>
- (a) Hariharan, P. C.; Pople, J. A. *Theor. Chim. Acta* **1973**, *28*, 213–222; (b) Francl, M. M.; Pietro, W. J.; Hehre, W. J.; Binkley, J. S.; Gordon, M. S.; DeFrees, D. J.; Pople, J. A. *J. Chem. Phys.* **1982**, *77*, 3654–3665.
- González, C.; Schlegel, H. B. *J. Phys. Chem.* **1990**, *94*, 5523–5527.
- MORPHY98, a program written by P.L.A. Popelier with a contribution from R.G.A. Bone, UMIST, Manchester, England, EU (1998). See also: Popelier, P. *Comput. Phys. Commun.* **1998**, *108*, 180–190.
- Popelier, P. L. A. *Chem. Phys. Lett.* **1994**, *228*, 160–164.
- (a) Shiro, M.; Yamakawa, M.; Kubota, T. *Acta Crystallogr., Sect. B: Struct. Sci.* **1979**, *35*, 712–716; (b) Stoyanovich, F. M.; Krayushkin, M. M.; Mamaeva, O. O.; Yufit, D. S.; Struchkov, Yu. T. *Gazz. Chim. Ital.* **1993**, *123*, 39–44; (c) Groundwater, P. W.; Nyerges, M.; Fejes, I.; Hibbs, D. E.; Bendell, D.; Anderson, R. J.; McKillop, A.; Sharif, T.; Zhang, W. *ARKIVOC* **2000**, *1*, 684–697.
- Kim, J.-N.; Ryu, E.-K. *Tetrahedron Lett.* **1993**, *34*, 3567–3570.

17. Dvorak, M. A.; Ford, R. S.; Suenram, R. D.; Lovas, F. J.; Leopold, K. R. *J. Am. Chem. Soc.* **1992**, *114*, 108–115.
18. Swanson, B.; Shriver, D. F.; Ibers, J. A. *Inorg. Chem.* **1969**, *8*, 2182–2189.
19. Giesen, D. J.; Phillips, J. A. *J. Phys. Chem. A* **2003**, *107*, 4009–4018.
20. Vijay, A.; Sathyanarayana, D. N. *J. Phys. Chem.* **1996**, *100*, 75–84.
21. (a) Emeleus, H. J.; Wade, K. *J. Chem. Soc.* **1960**, 2614–2617; (b) Laubengayer, A. W.; Sears, D. S. *J. Am. Chem. Soc.* **1945**, *67*, 164–167.
22. (a) Watari, F. *J. Phys. Chem.* **1980**, *84*, 448–452; (b) Devarajan, V.; Cyvin, S. J. *Z. Naturforsch., A: Phys. Sci.* **1971**, *26*, 1346; (c) Swanson, B.; Shriver, D. F. *Inorg. Chem.* **1970**, *9*, 1406–1416.
23. For selected recent examples, see: (a) Molteni, G.; Ponti, A. *Chem.—Eur. J* **2003**, *9*, 2770–2774; (b) Ess, D. H.; Houk, K. N. *J. Phys. Chem. A* **2005**, *109*, 9542–9553; (c) Freeman, F.; Dang, P.; Huang, A. C.; Mack, A.; Wald, K. *Tetrahedron Lett.* **2005**, *46*, 1993–1995.
24. Sustmann, R. *Tetrahedron Lett.* **1971**, *12*, 2717–2720.
25. (a) Bader, R. F. W. *Atoms in Molecules: A Quantum Theory*; Clarendon: Oxford, UK, 1990; (b) Bader, R. F. W. *Acc. Chem. Res.* **1985**, *18*, 9–15; (c) Wiberg, K. B.; Bader, R. F. W.; Lau, C. D. H. *J. Am. Chem. Soc.* **1987**, *109*, 985–1001.
26. Ebrahimi, A.; Roohi, H.; Habibi, M.; Karimian, T.; Vaziri, R. *Chem. Phys. Lett.* **2006**, *419*, 179–183.
27. Alsberg, B. K.; Marchand-Geneste, N.; King, R. D. *Anal. Chim. Acta* **2001**, *446*, 3–13.
28. Lopez, J. L.; Mandado, M.; Grana, A. M.; Mosquera, R. A. *Int. J. Quantum Chem.* **2002**, *86*, 190–198.
29. Aray, Y.; Murgich, J.; Luna, M. A. *J. Am. Chem. Soc.* **1991**, *113*, 7135–7143.
30. (a) Kanemasa, S.; Nishiuchi, M. *Tetrahedron Lett.* **1993**, *34*, 4011–4014; (b) Kanemasa, S.; Kobayashi, S. *Bull. Chem. Soc. Jpn.* **1993**, *66*, 2685–2693; (c) Kanemasa, S.; Nishiuchi, M.; Kamimura, A.; Hori, K. *J. Am. Chem. Soc.* **1994**, *116*, 2324–2339; (d) Kanemasa, S.; Okuda, K.; Yamamoto, H.; Kaga, S. *Tetrahedron Lett.* **1997**, *38*, 4095–4098; (e) Yamamoto, H.; Watanabe, S.; Kadotani, K.; Hasegawa, M.; Noguchi, M.; Kanemasa, S. *Tetrahedron Lett.* **2000**, *41*, 3131–3136; (f) Kamimura, A.; Kaneko, Y.; Ohta, A.; Matsuura, K.; Fujimoto, Y.; Kakehi, A.; Kanemasa, S. *Tetrahedron* **2002**, *58*, 9613–9620; (g) Yamamoto, H.; Watanabe, S.; Hasegawa, M.; Noguchi, M.; Kanemasa, S. *J. Chem. Res., Synop.* **2003**, 284–286; (h) Mičuch, P.; Fišera, L.; Cyrański, M. K.; Krygowski, T. M.; Krajčák, J. *Tetrahedron* **2000**, *56*, 5465–5472.
31. Sibi, M. P.; Itoh, K.; Jasperse, C. P. *J. Am. Chem. Soc.* **2004**, *126*, 5366–5367.
32. (a) Ukaji, Y.; Sada, K.; Inomata, K. *Chem. Lett.* **1993**, 1847–1850; (b) Shimizu, M.; Ukaji, Y.; Inomata, K. *Chem. Lett.* **1996**, 455–456; (c) Ukaji, Y.; Katsunori, K.; Inomata, K. *Chem. Lett.* **1997**, 547–548; (d) Ishida, Y.; Ukaji, Y.; Fujinami, S.; Inomata, K. *Chem. Lett.* **1998**, 1023–1024.
33. Faita, G.; Paio, A.; Quadrelli, P.; Rancati, F.; Seneci, P. *Tetrahedron* **2001**, *57*, 8313–8322.
34. Fukuda, S.; Kamimura, A.; Kanemasa, S.; Hori, K. *Tetrahedron* **2000**, *56*, 1637–1647.